molecular pharmaceutics

ARTICLE

pubs.acs.org/molecularpharmaceutics

Role of α-Relaxation on Crystallization of Amorphous Celecoxib above T_g Probed by Dielectric Spectroscopy

Ajay K. R. Dantuluri, Aeshna Amin, Vibha Puri, and Arvind K. Bansal*

National Institute of Pharmaceutical Education and Research (NIPER), Sector 67, SAS Nagar (Mohali), Punjab 160 062, India

ABSTRACT: In the present study, the role of α-relaxation toward isothermal crystallization of amorphous celecoxib was studied using dielectric spectroscopy (DES). The dielectric response of the α-relaxation was measured as a function of frequency (10^{-1} to 10^6 Hz), isothermally at every 4 K interval in the range of 303.15 to 443.15 K. The dielectric loss spectrum at each temperature was analyzed using the Havriliak Negami (HN) equation to extract the characteristic relaxation time, τ_{HN}. Two Vogel−Fulcher−Tammann (VFT) functions were required for representing the temperature dependence of τ_{HN} across the temperature range of study. The VFT fit parameters obtained from the two regions varied drastically pointing toward the underlying differences in the dynamics of relaxation above and below the crossover. Later, *in situ* isothermal crystallization experiments were performed at 363.15, 368.15, 373.15, and 378.15 K. The conversion rate, obtained from the normalized dielectric strength, was modeled using the Avrami model, which indicated the possibility of different crystallization mechanism at higher crystallization temperatures. HN shape parameters, α_{HN} and product of α_{HN} and β_{HN}, were analyzed during the course of crystallization to understand the dynamics of amorphous phase when crystallites were being evolved. HN shape parameters indicated α-like motions were affected, whereas β-like remained unaffected by the crystallization temperature. Characteristic crystallization time, τ_{cr}, obtained from Avrami fits, showed Arrhenius type of temperature dependence ($R^2 = 0.999$). A plot between log τ_{cr} and log τ_{HN} show a linear regression with R^2 of 0.997 indicating the direct correlation between these two phenomena. However, the coupling coefficient was found to be varying within the temperature range of study, indicating tendency of crystallization to be more diffusion controlled at higher crystallization temperatures. With different crystalline solid phase crystallizing at higher crystallization temperature, complemented with direct correlation between log τ_{cr} and log τ_{HN}, Avrami modeling of crystallization and HN shape parameter analysis, the role of α-relaxation in the crystallization of amorphous celecoxib at $T > T_g$ is emphasized.

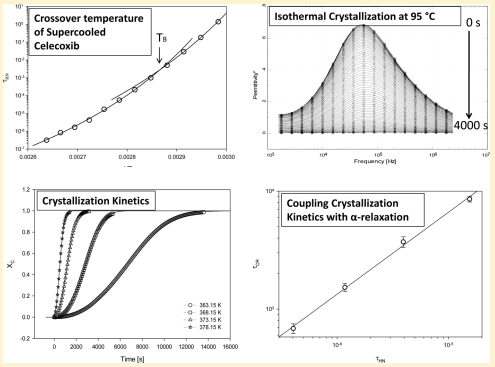

KEYWORDS: α-relaxation, VFT crossover, isothermal crystallization, HN shape parameters, Avrami model

INTRODUCTION

Recent years have witnessed an increasing number of molecules, with poor aqueous solubility, reaching the drug development pipeline. Amorphous systems by virtue of their higher free energy can help in improving the delivery of poorly water-soluble drugs. However, higher thermodynamic energy of an amorphous system compromises its physical and chemical stability. Nanocrystalline solid dispersions (NCSDs) have emerged as a viable alternative delivery platform for poorly water-soluble drugs. One way of generating NCSD involves annealing of amorphous solid dispersion.[1,2] It has been reported that crystallization is very slow below T_g with initial rapid crystallization attributing to surface crystallization followed by abrupt suspension of crystallization, thus resulting in partial crystalline samples.[3] Therefore, annealing above T_g is preferred for achieving NCSDs. Understanding mechanisms involved in nucleation and crystal growth above T_g would help in designing robust NCSDs with desirable properties like the size distribution of the nanocrystals.

To understand the mechanisms involved in nucleation and crystal growth, the dynamics of relaxation has often been correlated to crystallization. Dynamics of relaxation is often represented by structural relaxation time (i.e., molecular mobility). Molecular motions, in general, are of two types, α- and β-like. α-Relaxation is the motions involved in the dynamics of glass transition and is generally considered to be low frequency cooperative motion of multiple molecules on a longer length scale. In contrast, β-mobility is considered to be high frequency noncooperative motion, which occurs on a smaller length scale.[4,5] α-like motions are generally constrained below T_g as the viscosity of the system increases drastically, and are usually considered to be negligible at temperatures far below T_g.[4] Recently, Grzbowska et al. characterized amorphous celecoxib using dielectric spectroscopy (DES) for different molecular relaxations (across the temperature) and studied isothermal crystallization at 293 K (below T_g). They acknowledged, based on the reported literature, that crystallization below T_g is ultimately affected by β-relaxation.[6] This

Received: November 30, 2010
Accepted: May 2, 2011
Revised: April 24, 2011
Published: May 02, 2011

study gave important leads in assessing physical stability of amorphous celecoxib below T_g, with respect to mechanism involved in crystallization. Alie et al. demonstrated Arrhenius type temperature dependence of both β-relaxation (below T_g) and the characteristic crystallization time, τ_{cr} (above T_g), of a model compound. Based on similar type of temperature dependence, they concluded molecular motions responsible for β-relaxation were contributing to the crystallization process.[7] Attempts have also been made to correlate crystal growth and α-relaxation times, below and above T_g, to delineate the mechanisms involved in the crystallization of amorphous systems,[8−10] and the correlation between these two was found to be reasonable. Hence, molecular relaxations responsible for crystallization vary from case to case. Moreover, for the crystallization to be complete translational and/or rotational movement (α-relaxation) of the molecules, in order to become incorporated into the crystal structure (crystal growth), is as important as the exact configuration of molecules to form a critical nucleus (nucleation). The extrapolation of β-relaxation being the sole controlling factor for crystallization above T_g would not be appropriate because α-relaxations are not constrained above T_g unlike those observed at temperatures below T_g. The interplay between these two phenomena (nucleation and crystal growth) changes as a function of temperature with crystal growth predominating over all crystallization above T_g. Therefore, a comprehensive study of crystallization above T_g would be of great help in delineating the underlying mechanisms of crystallization and thus giving leads for designing controlled crystal growth.

With the advances in analytical tools, study of molecular motions, with respect to time and temperature scale, has become achievable. DES has been used for probing molecular motions in the supercooled and glassy state of various pharmaceuticals.[7,11−20] It has also been used for determining the kinetics of isothermal crystallization of amorphous systems,[21] including pharmaceuticals.[7] Kinetics of crystallization have been often used for explaining mechanisms of nucleation and crystal growth by fitting the conversion of amorphous to crystalline to Avrami law.[22−24]

The main objective of the present work was to study the α-relaxation process in a supercooled liquid pharmaceutical, as a function of temperature, and correlate it to crystallization behavior at temperatures above T_g. Celecoxib was selected as the model compound. Isothermal crystallization of the amorphous sample was monitored *in situ* in the dielectric cell with time. *In situ* crystallization studies enabled following molecular dynamics of supercooled liquid during isothermal crystallization. The kinetics of conversion, determined from Avrami model fitting, and shape parameters of the dielectric loss spectra during crystallization helped in delineating the mechanism of crystallization above T_g.

EXPERIMENTAL SECTION

Materials. Celecoxib (CLB), chemically 4-[5-(4-methylphenyl)-3-(trifluoromethyl)-1*H*-pryzol-1-yl]benzenesulfonamide (assay value >99%) polymorph III, was received as a gift sample from Zydus Cadila Healthcare Ltd. (Ahmedabad, India).

Methods. *Dielectric Measurements.* Dielectric measurements were carried out using a Novocontrol Concept 40 broadband dielectric spectrometer in the frequency range of 10^{-1} to 10^7 Hz. Relative humidity and temperature were controlled by purging compressed gas (dry air) connected to Quadro system, initialized for dry gas option. Temperature was controlled within ±0.05 K for isothermal measurements. The sample was placed into a dielectric cell specially designed for powder, liquids and low molecular weight systems exhibiting significant flow at higher temperatures.[25] Two strips of PTFE were placed along with the crystalline sample. These strips were kept to ensure constant thickness of the molten sample during the analysis. Celecoxib was melted in the dielectric cell by heating to 458.15 K and upper electrode was places onto PTFE strips. Then the dielectric cell was heated again to 458.15 K and held isothermally for 10 min. Thereafter the cell was transferred to a vacuum desiccator and allowed to cool to room temperature. The glass formed at room temperature was subsequently subjected to dielectric measurements. A constant force on the upper electrode ensured good contact between the sensor and sample throughout experiment.

Temperature Dependence of Dielectric Relaxation. The dielectric response as a function of frequency (10^{-1} to 10^7 Hz) was recorded isothermally for various temperatures. The temperature ranges employed were from 307.15 to 443.15 at 4 K.

Isothermal Crystallization Studies. In situ isothermal crystallization studies were performed at 363.15, 368.15, 373.15, and 378.15 K using a Novocontrol Concept 40 broadband dielectric spectrometer. The frequency range of the scan at each crystallization temperature was adjusted to scan only the dielectric loss of α-relaxation at the respective temperature. The dielectric response as a function of frequency was collected continuously at 1 min intervals until the amorphous system crystallized completely.

Solid-Phase Characterization. Powder X-ray Diffraction (PXRD). PXRD patterns were recorded at room temperature using Bruker's model D8 Advance diffractometer (Karlsruhe, West Germany) equipped with a compensating slit, using Cu K radiation at 40 kV and 40 mA passing through nickel filter with divergence slit (0.5°), antiscattering slit (0.5°) and receiving slit (0.1 mm). Samples were scanned over a range of 2θ values from 3° to 40° at a scan rate of 0.01°/s. The recorded diffractograms were analyzed with DIFFRACplus EVA (ver. 9.0) diffraction software

Differential Scanning Calorimetry (DSC). DSC experiments were performed using a Q 2000 (TA Instruments, DE, USA) equipped with refrigerated cooling accessory. The DSC cell was purged with nitrogen at 50 mL/min. Indium was used to calibrate the temperature and cell constant. Accurately weighed samples (2−3 mg) in aluminum pans were scanned at a heating rate of 1 K/min. The data was analyzed using Universal Analysis 2000 software version 4.5A.

Microscopy. The powder samples obtained after isothermal crystallization were observed under Leica DMLP polarized microscope (Leica Microsystems Wetzlar GmbH, Wetzlar, Germany). Photomicrographs were acquired using a Leica DC 300 camera and analyzed using Leica IM 50 (version 1.20) software.

RESULTS

The present study was targeted at quantifying the relaxation dynamics of celecoxib in the supercooled liquid state and correlating it to its crystallization tendency. This was done by correlating the temperature dependent relaxation parameters of supercooled liquid celecoxib with isothermal crystallization kinetics.

Dielectric Relaxation of Amorphous Celecoxib. The dielectric response of amorphous celecoxib as a function of temperature (303.15 to 443.15 K) and frequency (10^{-1} to 10^7 Hz) was recorded. Dielectric relaxation, i.e, frequency dependent response in the dielectric spectra, was identified as a step change

in the real permittivity spectra and as a peak in the loss spectra, in the temperature region of 333.15 to 379.15 K. This response was attributed to the α-relaxations of amorphous celecoxib. The real and imaginary parts of the response were fitted to the Havriliak Negami (HN) function (eq 1) to obtain the mean relaxation time of the α-relaxation process at selected temperatures.

$$\varepsilon^*(\omega) = \varepsilon_\infty + \frac{\varepsilon_S - \varepsilon_\infty}{(1 + (i\omega\tau_{HN})^{\alpha_{HN}})^{\beta_{HN}}} \quad (1)$$

where τ_{HN} is a characteristic relaxation time that is related to the frequency of maximal loss f_{max}, $\Delta\varepsilon = \varepsilon_S - \varepsilon_\infty$ is the dielectric relaxation strength of the process under investigation and ε_∞ the high frequency limit of the real part $\varepsilon'(\omega)$; α_{HN} and β_{HN} are fractional shape parameters ($0 < \alpha_{HN} < 1$ and $0 < \beta_{HN} < 1$) describing the symmetric and asymmetric broadening of the dielectric spectrum. The shape parameter α_{HN} specifies the slope of the low frequency side of the relaxation peak in ε'', whereas $-\alpha_{HN}\beta_{HN}$ represents the slope of the high frequency side of the relaxation in ε''. Conductivity effects were taken into account by adding a contribution $(\sigma_{DC}/\varepsilon_0\omega)$ to the imaginary part of the fit function; σ_{DC} is the dc conductivity of the sample, and ε_0 is the dielectric permittivity of vacuum. Dielectric response of amorphous celecoxib was recorded for triplicate samples. RSD of τ_{HN} was found to be lesser than 3% at all determined temperature points.

The temperature dependence of characteristic relaxation time, τ_{HN}, is usually defined by the Vogel−Fulcher−Tammann (VFT) law (eq 2)

$$\tau(T) = \tau_0 \exp\left[\frac{E_a}{k_B(T - T_0)}\right] \quad (2)$$

where $\tau(T)$ relaxation is τ_{HN} obtained by fitting the permittivity to the HN function at temperature T, τ_0 is the pre-exponential factor (usually 10^{-14}), E_a is the activation energy of the relaxation, k_B is the Boltzmann constant and T_0 is the Vogel temperature. A single VFT fit was insufficient to explain the α-relaxation for amorphous celecoxib across the temperature range. Two VFT fits were used to define the temperature dependence of α-relaxation. A low temperature VFT fit crossed over to high temperature VFT fit at a temperature, T_B, as presented in Figure 1. RSD for the VFT fit parameters, τ_0, E_a, and T_0 for each temperature range were found to be lesser than 5%. Reports of such VFT crossovers are sparse in the pharmaceutical literature. Apart from the present case of celecoxib, ibuprofen[18] is the only other instance of a pharmaceutical active exhibiting a VFT crossover.

The present article deals with crystallization at temperatures above T_B, in the range of 363.15 to 378.15 K. High temperature VFT fit was used for correlating to the isothermal crystallization. A detailed investigation of mechanisms involved in VFT crossover behavior and its influence on crystallization above and below T_B forms a subject matter of future study.

Isothermal Crystallization. Isothermal crystallization of celecoxib was investigated at temperatures 363.15, 368.15, 373.15, and 378.15 K, using a dielectric spectrometer. The validity of using DES measurements for quantifying crystallization has been previously proposed and checked for different glassy materials.[26] The same was found to comply in the present study and will be discussed in the subsequent sections. The isothermal dielectric response of amorphous celecoxib was measured continuously at 1 min intervals throughout the course of crystallization. The frequency range at each temperature, used in the isothermal crystallization study, was limited to the onset and end set of the α-relaxation peak to minimize the time of each frequency sweep. A representative plot of dielectric response (real and imaginary permittivity as a function of log frequency) of supercooled liquid celecoxib, during the course of crystallization at 368.15 K, is presented in the Figure 2.

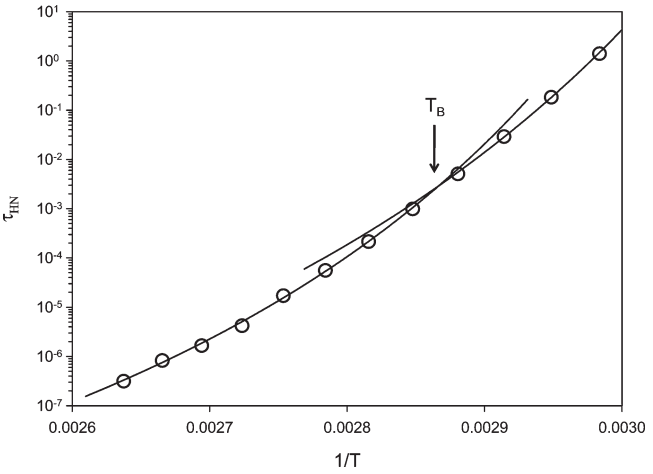

Figure 1. Two VFT fits (low temperature and high temperature) describing temperature dependence of τ_{HN}, crossing over at T_B.

The dielectric response at each time was fitted to the HN function to obtain the dielectric strength ($\Delta\varepsilon$), relaxation time (τ_{HN}), α_{HN} and β_{HN}. Reduction of the dielectric strength is considered as the measure of decrease in amorphous fraction in the sample. A normalized dielectric strength was used for quantifying the fraction crystallized, as dielectric strength varies at different temperatures (eq 3).

$$X_C = 1 - \frac{\Delta\varepsilon_{(t)}}{\Delta\varepsilon_{(t=0)}} \quad (3)$$

The τ_{HN}, obtained from HN fitting of isothermal dielectric response, when plotted against the degree of crystallization, remained almost constant, until $X_C > 0.9$ (Figure 3), thus indicating negligible influence of evolving crystallites on the relaxation f_{max} of the amorphous celecoxib. This validated the use of DES measurements for quantifying the amorphous content of celecoxib, during the course of crystallization. The conversion of amorphous to crystalline state at different temperatures is presented in Figure 4.

Modeling of Crystallization Kinetics. Kinetics of crystallization is widely treated with the Avrami model for understanding the mechanisms of nucleation and crystal growth. The conversion of amorphous to crystalline state ($X_C(t)$) as a function of time, t (obtained from the dielectric measurements), was modeled to the following Avrami expression (eq 4).

$$X_C(t) = 1 - \exp(-kt^n) \quad (4)$$

where k is the temperature dependent rate constant and n can vary from 1 to 7, based on the nucleation type and crystal growth mechanisms during the course of conversion. It has been widely acknowledged that a single Avrami model is insufficient to fit the conversion for entire time scale (from 0 to 100% conversion), as the crystallization rates in the initial and final stages are very low.[21,23]

The Avrami equation (eq 5) was refined to include the induction time, which is a characteristic time required for initiation of

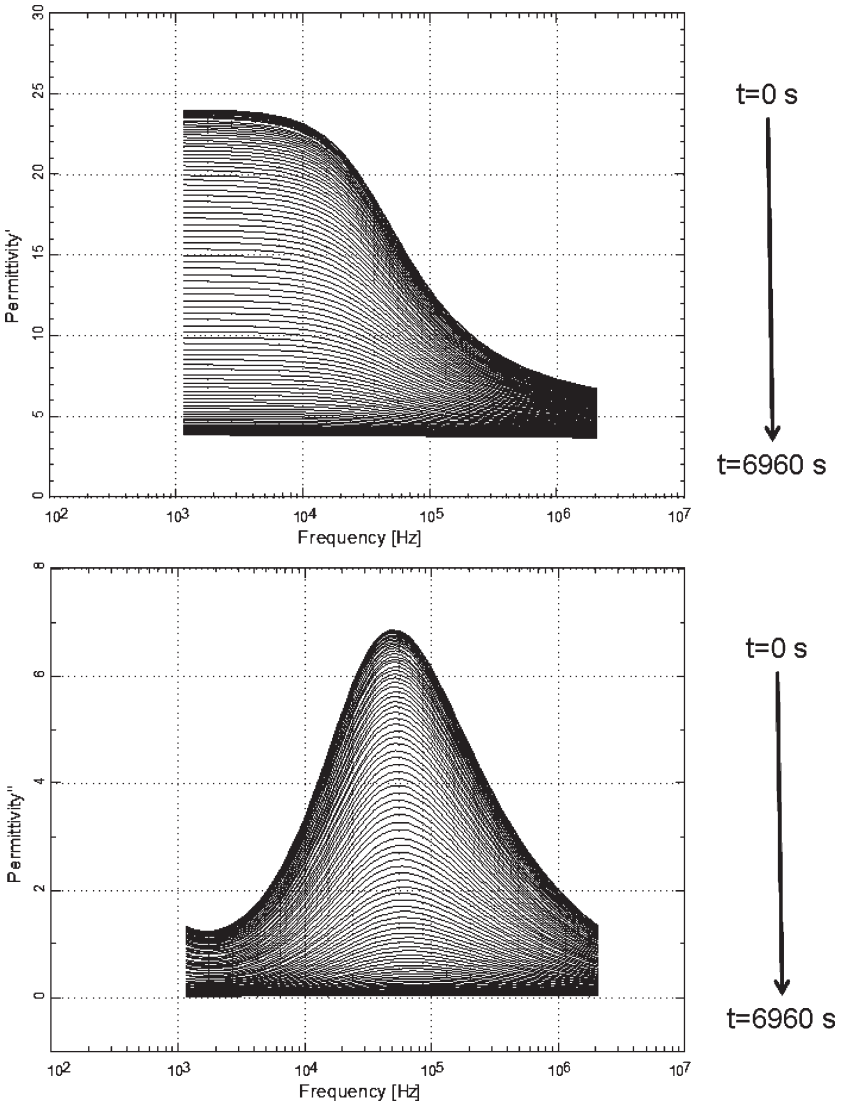

Figure 2. Frequency dependence of isothermal dielectric measurements: (top) real part and (bottom) imaginary part of complex permittivity recorded at 368.15 K for 90 min, at intervals of 1 min.

the isothermal crystallization,

$$X_C(t) = 1 - \exp\left[-\left(\frac{t - t_0}{\tau_{cr}}\right)^n\right] \quad (5)$$

where t_0, τ_{cr} and n are induction time, characteristic crystallization time and Avrami exponent, respectively. Equation 5 is a modified method of data analysis proposed by Avramov et al.[27] The conversion of amorphous to crystalline at all the crystallization temperatures is presented in Figure 4 with the solid line representing the Avrami fit. The fitting parameters of the isothermal crystallization to eq 5 are presented in Table 1.

Higher standard deviations in the induction time, t_0, can be due to the fitting of entire conversion range (0 to 1) with a single Avrami model, which may not be appropriate since the crystallization in the initial and final stages is fairly invariant. However, in the present work, the objective of the model fitting was to obtain τ_{cr} and the Avrami exponent, n. It was observed that at 363.15 and 368.15 K, the n value is approximately the same and close to 3. However, it decreases to 2.68 and 2.21 with further increase in the crystallization temperature to 373.15 and 378.15 K.

Solid-Phase Analysis. Crystalline solids obtained after the isothermal crystallization at the four temperatures were collected individually and ground gently using mortar and pestle to obtain a powder. The solid phases were characterized using PXRD, DSC, TGA and polarized light microscopy. TGA showed no weight loss within the temperature range of 303.15 to 453.15 K, eliminating any chances of hydrates and solvates. DSC and PXRD overlay of solid phases obtained by isothermal crystallization at respective temperatures is presented in Figure 5 and Figure 6 respectively, and the results were compared to crystal forms in the literature.[28] PXRD indicated the crystalline forms, obtained at 363.15, 368.15, and 373.15 K, to be equivalent to the reported form I. However, the PXRD pattern of the crystalline form obtained at 378.15 K was different and had peaks of both form I and form II, implying that the solid phase is a mixture of two forms. Microscopy indicated no significant changes in the morphology among the crystalline solids obtained at different crystallization temperatures (Figure 7).

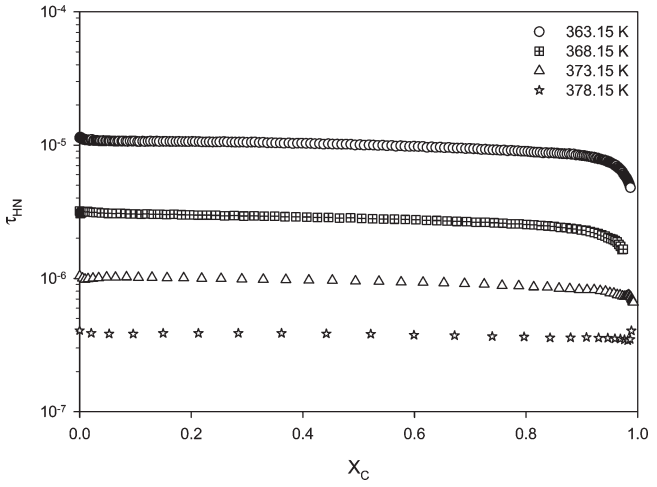

Figure 3. log τ_{HN} as a function of degree of crystallinity at respective crystallization temperatures.

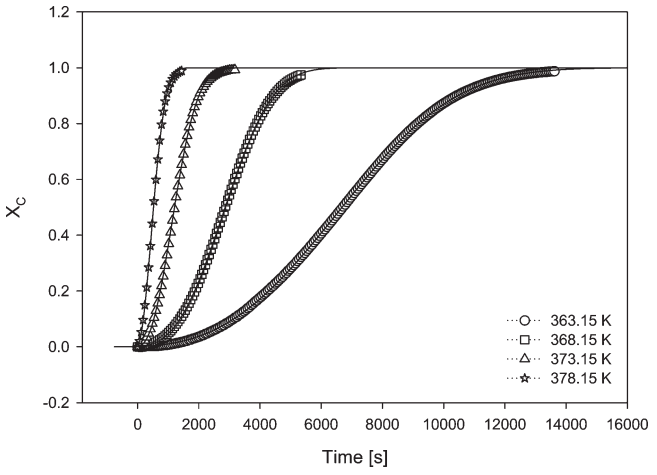

Figure 4. Degree of crystallinity as a function of time at different crystallization temperatures. Solid lines represent Avrami fits.

DISCUSSION

Trends of HN Shape Parameters during Isothermal Crystallization. The shape of the dielectric loss spectra as a function of frequency was analyzed in detail to understand the relaxation dynamics during the crystallization process. Increase in α_{HN} with increase in crystallization temperature was observed (as shown in Figure 8). A higher α_{HN}, at zero time, at higher temperature can be explained by α-like motions, being weakly cooperative, having uniform distribution of relaxation times with increase in temperature.[19] In other words, the distribution of the relaxing species is narrower at higher temperatures. Probing the dynamics of amorphous system during the crystallization would provide better insight into the role of different relaxation mechanisms, on crystallization.

Schonhals and Schlosser,[29] by applying the scaling hypothesis proposed by E. Donth and K. Schneider to the dielectric loss curve, put forward a model which indicates that high frequency tail is determined mainly by small scale modes and the low frequency tail by large scale modes. This empirical model is used

Table 1. Fit Parameters of Modified Avrami Fit Function[a]

temp (K)	t_0 (s)	τ_{cr} (s)	n
363.15	862.13 (498.82)	8552.87 (470.56)	2.98 (0.35)
368.15	425.91 (91.22)	3714.18 (379.23)	3.16 (0.11)
373.15	111.77 (74.51)	1525.79 (118.02)	2.68 (0.20)
378.15	56.66 (23.99)	683.97 (64.14)	2.21 (0.16)

[a] Data is represented as average (SD) for n = 3.

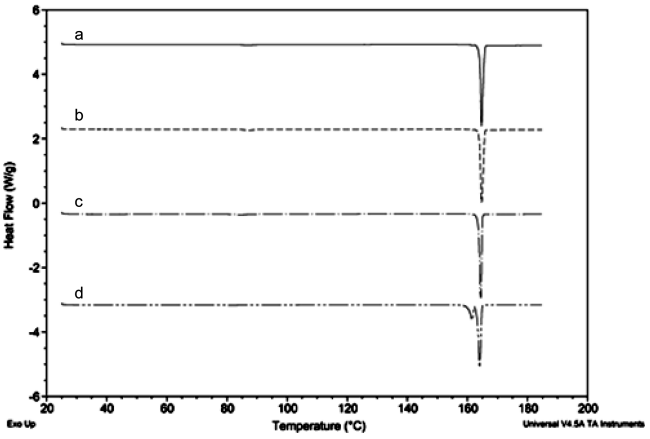

Figure 5. DSC overlay of solid phases crystallized at (a) 363.15 K, (b) 368.15 K, (c) 373.15 K and (d) 378.15 K.

to explain the dynamics of various amorphous polymeric systems during crystallization.[30−33] Though this model is explained in the context of polymers, the physical basis of the model, that cooperative global motions are considered as large scale molecular mobility (intermolecular interactions) and noncooperative local motions as small scale molecular mobility (intramolecular interactions), indicate the extendibility of the model to α-like and β-like motions in low molecular weight systems. Thus according to this model, changes in α_{HN} (slope of low frequency tail of dielectric loss curve) and product of α_{HN} and β_{HN} (negative slope of high frequency tail of dielectric loss curve) represent α-like and β-like motions respectively. To understand the dynamics of amorphous relaxations of celecoxib during the course of its crystallization at different temperatures, α_{HN} and product of α_{HN} and β_{HN} at representative time points were plotted against the degree of conversion (X_C) (Figure 8).

In the present study, temperature dependent change of trends in α_{HN} indicates changes in α-like motions, whereas no change in trends of product of α_{HN} and β_{HN} indicates unaltered trends in β-like motions with crystallization temperature. It was observed that, for the temperatures 363.15 and 368.15 K, α_{HN} decreased with progressing crystallization whereas, at 373.15 and 378.15 K, it showed an increasing trend. The product of α_{HN} and β_{HN} decreased for all four temperatures. The declining α_{HN} with progressing crystallization at 363.15 and 368.15 K can be attributed to interference evolving crystallites on cooperativity length. However, increase in α_{HN} with course of crystallization at higher temperatures, 373.15 and 378.15 K, is difficult to explain, as the evolving crystallites would interfere with cooperitivity here also. The increasing trend of α_{HN} would probably point toward the unaffected bulk relaxation at higher crystallization temperatures. This indicates the possibility of altered mechanism of

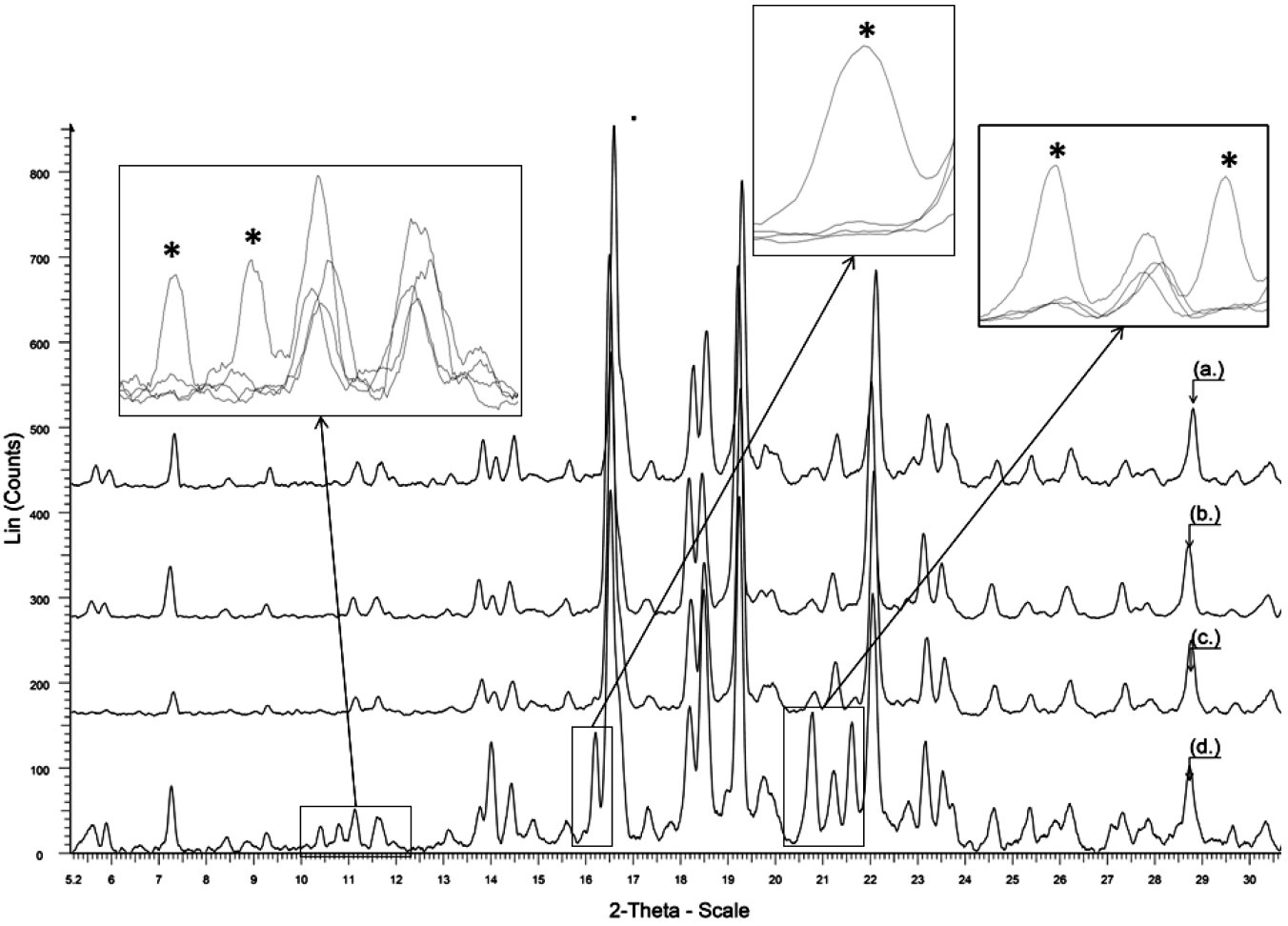

Figure 6. PXRD overlay of solid phases crystallized at (a) 363.15 K, (b) 368.15 K, (c) 373.15 K and (d) 378.15 K (insets show the extra peaks with * mark for solid crystallized at 378.15 K).

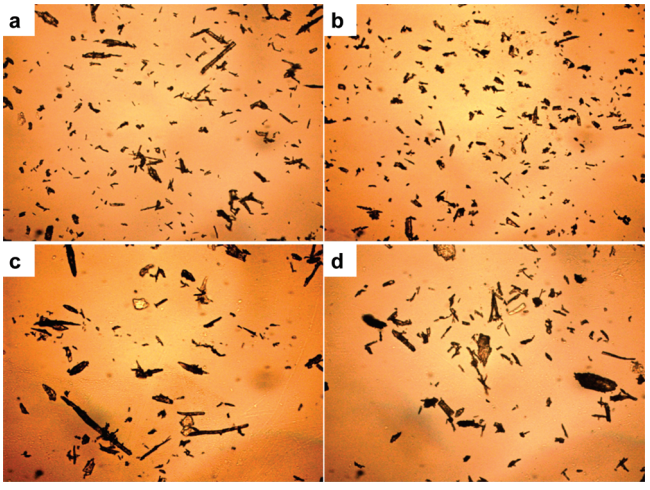

Figure 7. Microscopic photographs of solid phases crystallized at (a) 363.15 K, (b) 368.15 K, (c) 373.15 K and (d) 378.15 K.

crystallization at higher temperatures. A thorough understanding of mechanisms of nucleation and crystal growth is required to comprehend the course of dynamics of amorphous relaxations, as the crystallization progresses.

Crystallization Kinetics. The Avrami exponent is usually used as an indicator of crystal morphology. In general, an Avrami exponent of 3 indicates either (i) thermal nucleation and 2-dimensional growth or (ii) athermal nucleation and 3-dimensional growth. An Avrami exponent of 2 indicates either (i) thermal nucleation and 1-dimensional growth or (ii) athermal nucleation and 2-dimensional growth.

Microscopy showed no significant change in the crystal morphology of the recrystallized solid phases at different crystallization temperatures. This indicates the negligible differences in the crystal growth phase with crystallizing temperatures, signifying the possibility of differences in the nucleation phase of solid transformation. Therefore, decrease of Avrami exponent from ~3 to 2.21 with increase in crystallization temperature from 363.15 to 378.15 K is probably because of thermal nucleation at 363.15 and 368.15 K and nucleation tending to athermal nucleation at 373.15 and 378.15 K. Thermal nucleation, as it happens with time at a particular temperature, is often considered to happen homogeneously throughout the system.[34] In contrast athermal nucleation can be concentrated in certain regions of the system, followed by diffusion controlled crystal growth. Microscopy revealed presence of agglomerates and larger crystals at higher temperatures, thus supporting this hypothesis.

Correlation of Relaxation Dynamics of Amorphous Celecoxib with Crystallization. The main objective of the present

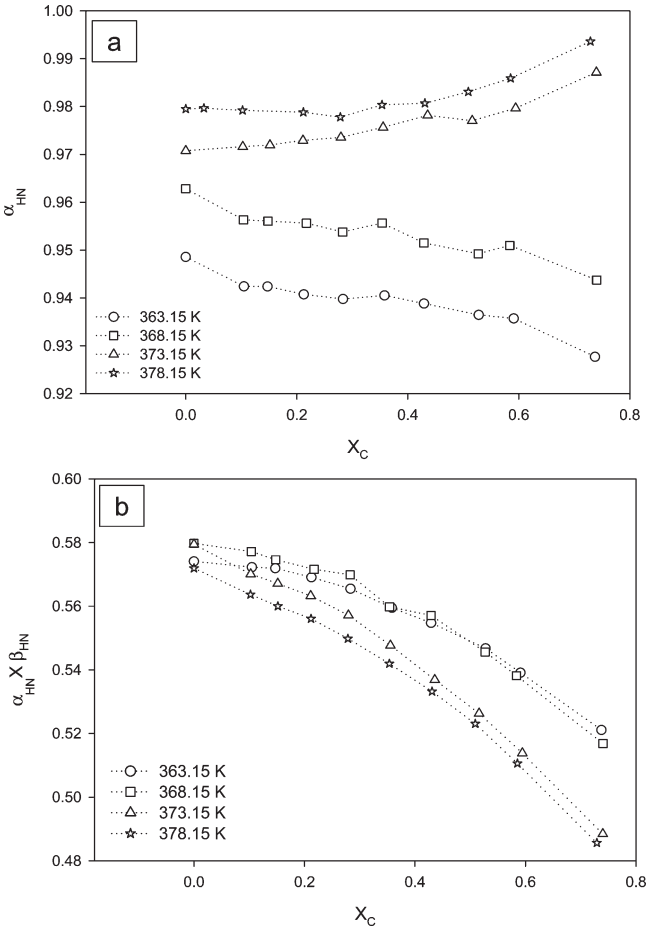

Figure 8. Trends of HN shape parameters (a) α_{HN} and (b) product of α_{HN} and β_{HN} during course of crystallization at respective temperatures.

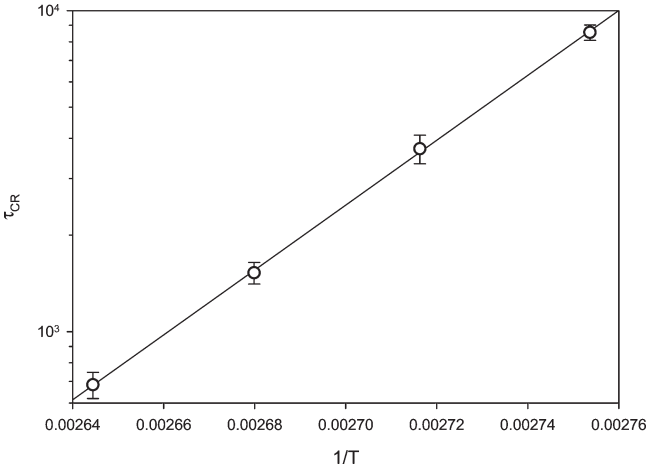

Figure 9. Temperature dependence of characteristic crystallization time, τ_{cr}.

study was to correlate the dynamics of amorphous relaxations with the crystallization process. Previous reports that have attempted such a correlation have presented the Arrhenius dependence of the characteristic crystallization time τ_{cr}. It was also shown that the crystal growth process above T_g seems be controlled by the

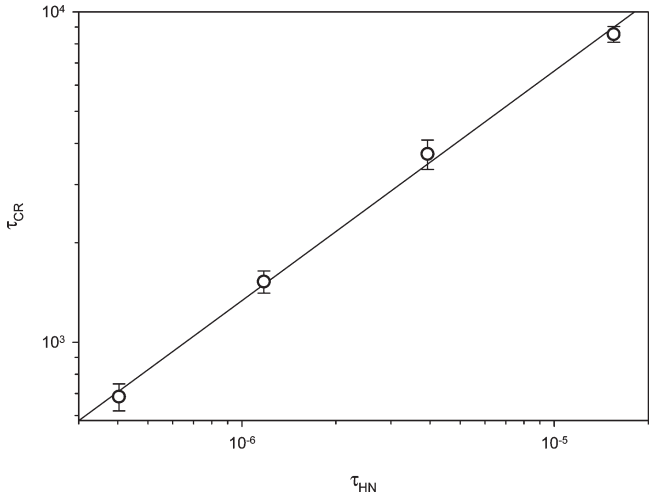

Figure 10. log−log plot of characteristic crystallization time, τ_{cr}, as a function of characteristic dielectric relaxation time, τ_{HN}.

intramolecular motions involving the β-relaxation mode and not by the molecular motions responsible for the α-relaxation mode.[7]

Figure 9 shows log τ_{cr} (obtained from the Avrami model fitting) plotted against the inverse of temperature. τ_{cr} showed a good Arrhenius dependence of temperature (R^2 0.9997). Conventionally, α-relaxation time and the characteristic crystallization time are correlated by plotting both the terms in the log−log scale. A slope, also referred to as coupling coefficient, of 1 indicates a diffusion controlled crystallization process,[8−10,35] and a decrease of slope from 1 indicates the differences in temperature dependence of the viscosity and diffusion of the sample. A plot of data of the present study gave a slope of 0.70 with regression coefficient, R^2, of 0.9974 (Figure 10). Removal of the data point of 363.15 K from the plot increased the slope to 0.75 and R^2 to 1. A *t* test, using SigmaPlot Windows Version 11.0, indicated significant statistical difference at $p = 0.024$ between the coupling coefficients 0.7 and 0.75. The significant change of slope with further narrowing of temperature range indicated that isothermal crystallization is controlled by diffusion differently, even within the temperature range of study. Crystallization of celecoxib became more diffusion controlled as the temperature range changed from 363.15−378.15 K to 368.15−378.15 K.

Further, the linear fit between these two, contradicts the VFT temperature dependence of τ_{HN}. This can be due to the temperature range of the present study. It has been reported that, far from T_g, the temperature dependence of τ_{HN} becomes weaker and tends toward Arrhenius dependence.[19] A decrease of slope from 1 indicates that the crystallization is moving away from a diffusion controlled process. This can be explained as differences of temperature dependence of τ_{cr} and the diffusion (which is reflected by τ_{HN} of α-relaxation) of the sample. The data of the present work represents that the dependence of crystallization on diffusion decreases as the temperature decreases and approaches T_g. At lower crystallization temperature, 363.15 K, the dependency of crystallization on α-relaxation is decreased as indicated by significant reduction of slope on inclusion of this data point in the analysis.

Keeping in view the findings of HN shape parameter analysis (Figure 8), Avrami modeling (Table 1) and coupling dielectric relaxation with crystallization time (Figure 10), the following

mechanistic understanding of crystallization behavior of celecoxib can be proposed:

1. At lower temperatures (363.15 and 368.15 K), a decrease in α_{HN} shape parameters during the course of crystallization indicates that the α-relaxations are hampered, as crystallization progresses. This lowers the contribution of the diffusion component toward crystallization as reflected by a lower coupling coefficient when the 363.15 K data point is included in a log−log plot of τ_{HN} vs τ_{cr}. Crystallization at these lower temperatures is characterized by uniform distribution of the evolving crystals and the longer cooperativity. An Avrami exponent, *n*, of 3 and microscopic observation at these two temperatures also confirm homogeneous crystallization throughout the sample.
2. At higher temperatures (373.15 and 378.15 K), the increasing trend of α_{HN} indicates that α-like motions were not affected during the course of crystallization. This can be attributed to shorter cooperativity and narrower distribution of relaxation species. This resulted in a higher contribution of the diffusion component toward crystallization, as reflected by a higher coupling coefficient when only higher temperatures were considered. This is also indicative of nonhomogeneous distribution of nuclei in the sample. The lower Avrami exponent also supports the above inference.

The phenomenon of mixture of forms being obtained at 378.15 K can be attributed to faster crystallization kinetics causing emergence of a lower melting form of celecoxib as per Ostwald's rule of stages. Moreover, an Avrami exponent of 2.26 at 378.15 K has been attributed to athermal nucleation followed by 2-dimensional growth. Hence, crystallization is predominantly controlled by crystal growth in the sample. The latter is further supported by the fact of crystallization being predominantly controlled by α-relaxation, as reflected by an increase in the coupling coefficient when only higher temperatures (368.15, 373.15, and 378.15 instead of 363.15, 368.15, 373.15 and 378.15) are considered.

The present study highlighted the importance of HN shape parameter analysis in understanding the mechanisms involved in the crystallization of amorphous phase. The change in the dynamics of the supercooled region above and below T_B opens an interesting area of isothermal crystallization research. The understanding of mechanisms involved in the crystallization can help in both stabilizing the amorphous form, by giving inputs for careful selection of stabilizing excipients, and designing NCSDs prepared by annealing the amorphous solid dispersions.

CONCLUSION

In the present study, dielectric spectroscopy (DES) was used to characterize α-relaxation in the supercooled liquid region and to correlate it to the crystallization tendency of celecoxib. The relaxation time, τ_{HN}, of the α-process showed Vogel−Fulcher−Tammann (VFT) type of temperature dependence. Two different VFT fits in the lower and higher temperature regions, demarcated by a crossover temperature T_B, were required to represent the temperature dependence of α-relaxation. Higher temperature VFT fit was used for correlating α-relaxation to the isothermal crystallization, as the crystallization experiments were performed above T_B. Isothermal crystallization studies of amorphous celecoxib were performed at different temperatures above T_B (363.15, 368.15, 373.15, and 378.15 K) with *in situ* dielectric measurements. The kinetics of conversion was modeled with the Avrami law for probing the differences in nucleation and crystal growth mechanism and extracting the characteristic crystallization time, τ_{cr}. The Avrami model parameter, *n*, decreased with increasing crystallization temperature indicating variations in the mechanisms involved in crystallization with temperature. τ_{cr} was found to have Arrhenius temperature dependence. Further, τ_{cr} was correlated with τ_{HN}, to investigate the contribution of diffusion on crystallization. Diffusion control on the crystallization varied even within the temperature range of study. The Havriliak Negami shape parameters, obtained from dielectric loss in the course of crystallization, also showed that the trend of α-like motions during the course of crystallization was affected differently by the crystallization temperature, whereas the trend of *β*-like motions was unchanged with temperature. Inferences drawn from the results and data analysis were able to explain the altered mechanisms of crystallization of amorphous celecoxib at different crystallization temperatures of the study and its overall dependence on the dynamics of α-like motions typified by the α-relaxation.

AUTHOR INFORMATION

Corresponding Author

*Department of Pharmaceutics. National Institute of Pharmaceutical Education and Research (NIPER), Sector 67, SAS Nagar (Mohali), Punjab 160 062, India. Phone: +91 172 2214682. Fax: +91 172 214692. E-mail: akbansal@niper.ac.in.

ACKNOWLEDGMENT

A.K.R.D. acknowledges Department of Biotechnology (DBT, New Delhi, India) for providing a senior research fellowship (Grant Ref. No. BT/PR10084/NNT/28/98/2007).

REFERENCES

(1) Yin, S. X.; Franchini, M.; Chen, J.; Hsieh, A.; Jen, S.; Lee, T.; Hussain, M.; Smith, R. Bioavailability Enhancement of a COX-2 Inhibitor, BMS-347070, from a Nanocrystalline Dispersion Prepared by Spray-Drying. *J. Pharm. Sci.* **2005**, *94*, 1598–1607.

(2) Qian, F.; Tao, J.; Desikan, S.; Hussain, M.; Smith, R. Mechanistic Investigation of Pluronic® Based Nano-Crystalline Drug-Polymer Solid Dispersions. *Pharm. Res.* **2007**, *24*, 1551–1560.

(3) Wu, T.; Yu, L. Surface Crystallization of Indomethacin Below T_g. *Pharm. Res.* **2006**, *23*, 2350–2355.

(4) Vyazovkin, S.; Dranca, I. Physical Stability and Relaxation of Amorphous Indomethacin. *J. Phys. Chem. B* **2005**, *109*, 18637–18644.

(5) Bhugra, C.; Pikal, M. J. Role of Thermodynamic, Molecular, and Kinetic Factors in Crystallization from the Amorphous State. *J. Pharm. Sci.* **2008**, *97*, 1329–1349.

(6) Grzybowska, K.; Paluch, M.; Grzybowski, A.; Wojnarowska, Z.; Hawelek, L.; Kolodziejczyk, K.; Ngai, K. L. Molecular Dynamics and Physical Stability of Amorphous Anti-Inflammatory Drug: Celecoxib. *J. Phys. Chem. B* **2010**, *114*, 12792–12801.

(7) Alie, J.; Menegotto, J.; Cardon, P.; Duplaa, H.; Caron, A.; Lacabanne, C.; Bauer, M. Dielectric Study of the Molecular Mobility and the Isothermal Crystallization Kinetics of an Amorphous Pharmaceutical Drug Substance. *J. Pharm. Sci.* **2004**, *93*, 218–233.

(8) Caron, V.; Bhugra, C.; Pikal, M. J. Prediction Of Onset Of Crystallization In Amorphous Pharmaceutical Systems: Phenobarbital, Nifedipine/PVP, And Phenobarbital/PVP. *J. Pharm. Sci.* **2010**, *99*, 3887–3900.

(9) Korhonen, O.; Bhugra, C.; Pikal, M. J. Correlation between Molecular Mobility and Crystal Growth of Amorphous Phenobarbital

and Phenobarbital with Polyvinylpyrrolidone and L-Proline. *J. Pharm. Sci.* **2008**, *97*, 3830–3841.

(10) Bhugra, C.; Shmeis, R.; Krill, S. L.; Pikal, M. J. Prediction of Onset of Crystallization from Experimental Relaxation Times. II. Comparison between Predicted and Experimental Onset Times. *J. Pharm. Sci.* **2008**, *97*, 455–472.

(11) Wojnarowska, Z.; Adrjanowicz, K.; Wlodarczyk, P.; Kaminska, E.; Kaminski, K.; Grzybowska, K.; Wrzalik, R.; Paluch, M.; Ngai, K. L. Broadband Dielectric Relaxation Study at Ambient and Elevated Pressure of Molecular Dynamics of Pharmaceutical: Indomethacin. *J. Phys. Chem. B* **2009**, *113*, 12536–12545.

(12) Duddu, S. P.; Sokoloski, T. D. Dielectric Analysis in the Characterization of Amorphous Pharmaceutical Solids. 1. Molecular Mobility in Poly(vinylpyrrolidone)-Water Systems in the Glassy State. *J. Pharm. Sci.* **1995**, *84*, 773–776.

(13) Johari, G. P.; Kim, S.; Shanker, R. M. Dielectric Relaxation and Crystallization of Ultraviscous Melt and Glassy States of Aspirin, Ibuprofen, Progesterone, and Quinidine. *J. Pharm. Sci.* **2007**, *96*, 1159–1175.

(14) Adrjanowicz, K.; Kaminski, K.; Paluch, M.; Wlodarczyk, P.; Grzybowska, K.; Wojnarowska, Z.; Hawelek, L.; Sawicki, W.; Lepek, P.; Lunio, R. Dielectric Relaxation Studies and Dissolution Behavior of Amorphous Verapamil Hydrochloride. *J. Pharm. Sci.* **2010**, *99*, 828–839.

(15) Johari, G. P.; Kim, S.; Shanker, R. M. Dielectric Studies of Molecular Motions in Amorphous Solid and Ultraviscous Acetaminophen. *J. Pharm. Sci.* **2005**, *94*, 2207–2223.

(16) Carpentier, L.; Decressain, R.; Desprez, S.; Descamps, M. Dynamics of the Amorphous and Crystalline α-, γ-Phases of Indomethacin. *J. Phys. Chem. B* **2006**, *110*, 457–464.

(17) Adrjanowicz, K.; Wojnarowska, Z.; Wlodarczyk, P.; Kaminski, K.; Paluch, M.; Mazgalski, J. Molecular Mobility in Liquid and Glassy States of Telmisartan (Tel) Studied by Broadband Dielectric Spectroscopy. *Eur. J. Pharm. Sci.* **2009**, *38*, 395–404.

(18) Bras, A. R.; Noronha, J. P.; Antunes, A. M.; Cardoso, M. M.; Schonhals, A.; Affouard, F.; Dionisio, M.; Correia, N. T. Molecular Motions in Amorphous Ibuprofen as Studied by Broadband Dielectric Spectroscopy. *J. Phys. Chem. B* **2008**, *112*, 11087–11099.

(19) Carpentier, L.; Decressain, R.; De Gusseme, A.; Neves, C.; Descamps, M. Molecular Mobility in Glass Forming Fananserine: A Dielectric, NMR, and TMDSC Investigation. *Pharm. Res.* **2006**, *23*, 798–805.

(20) Kaminski, K.; Kaminska, E.; Adrjanowicz, K.; Grzybowiska, K.; Wlodarczyk, P.; Paluch, M.; Burian, A.; Ziolo, J.; Lepek, P.; Mazgalski, J.; Sawicki, W. Dielectric Relaxation Study on Tramadol Monohydrate and its Hydrochloride Salt. *J. Pharm. Sci.* **2010**, *99*, 94–106.

(21) Viciosa, M. T.; Correia, N. T.; Salmeron Sanchez, M.; Carvalho, A. L.; Romao, M. J.; Gomez Ribelles, J. L.; Dionisio, M. Real-Time Monitoring of Molecular Dynamics of Ethylene Glycol Dimethacrylate Glass Former. *J. Phys. Chem. B* **2009**, *113*, 14209–14217.

(22) Khawam, A.; Flanagan, D. R. Basics and Applications of Solid-State Kinetics: A Pharmaceutical Perspective. *J. Pharm. Sci.* **2006**, *95*, 472–498.

(23) Zhou, D.; Schmitt, E. A.; Zhang, G. G.; Law, D.; Vyazovkin, S.; Wight, C. A.; Grant, D. J. Crystallization Kinetics of Amorphous Nifedipine Studied by Model-Fitting And Model-Free Approaches. *J. Pharm. Sci.* **2003**, *92*, 1779–1792.

(24) Khawam, A.; Flanagan, D. R. Solid-State Kinetic Models: Basics and Mathematical Fundamentals. *J. Phys. Chem. B* **2006**, *110*, 17315–17328.

(25) He, R.; Craig, D. Q. An Investigation into the Thermal Behaviour of an Amorphous Drug Using Low Frequency Dielectric Spectroscopy and Modulated Temperature Differential Scanning Calorimetry. *J. Pharm. Pharmacol.* **2001**, *53*, 41–48.

(26) Bras, A. R.; Viciosa, M. T.; Wang, Y.; Dionisio, M.; Mano, J. Crystallization of Poly(L-lactic acid) Probed with Dielectric Relaxation Spectroscopy. *Macromolecules* **2006**, *39*, 6513–6520.

(27) Avramov, I.; Avramova, K.; Rüssel, C. New Method to Analyze Data on Overall Crystallization Kinetics. *J. Cryst. Growth* **2005**, *285*, 394–399.

(28) Lu, G. W.; Hawley, M.; Smith, M.; Geiger, B. M.; Pfund, W. Characterization of a Novel Polymorphic Form of Celecoxib. *J. Pharm. Sci.* **2006**, *95*, 305–317.

(29) Schonhals, A.; Schlosser, E. Dielectric Relaxation In Polymeric Solids Part 1. A New Model for The Interpretation of the Shape of the Dielectric Relaxation Function. *Colloid Polym. Sci.* **1989**, *267*, 125–132.

(30) Sanz, A.; Nogales, A.; Ezquerra, T. A.; Soccio, M.; Munari, A.; Lotti, N. Cold Crystallization Of Poly(Trimethylene Terephthalate) as Revealed by Simultaneous WAXS, SAXS, And Dielectric Spectroscopy. *Macromolecules* **2009**, *43*, 671–679.

(31) Dendzik, Z.; Gburski, Z. Dielectric Spectroscopy Of Glass-Forming Polymer Poly(aryl ether ketone ketone) During Crystallization. *J. Mol. Struct.* **1997**, *410−411*, 237–240.

(32) Sics, I.; Ezquerra, T. A.; Nogales, A.; Balta-Calleja, F. J.; Kalnins, M.; Tupureina, V. On the Relationship between Crystalline Structure and Amorphous Phase Dynamics During Isothermal Crystallization of Bacterial Poly(3-hydroxybutyrate-co-3-hydroxyvalerate) Copolymers. *Biomacromolecules* **2001**, *2*, 581–587.

(33) Fukao, K.; Miyamoto, Y. Relaxation Behavior of α-Process of Poly(ethylene terephthalate) During Crystallization Process. *J. Non-Cryst. Solids* **1997**, *212*, 208–214.

(34) Smith, K. W.; Smith, P. R.; Furo, I.; Pettersson, E. T.; Cain, F. W.; Favre, L.; Talbot, G. Slow Recrystallization of Tripalmitoylglycerol from MCT Oil Observed by ^{2}H NMR. *J. Agric. Food. Chem.* **2007**, *55*, 8585–8588.

(35) Napolitano, S.; Wubbenhorst, M. Effect Of A Reduced Mobility Layer On the Interplay Between Molecular Relaxations and Diffusion-Limited Crystallization Rate in Ultrathin Polymer Films. *J. Phys. Chem. B* **2007**, *111*, 5775–5780.